Electronic Supplementary Material (ESI) for Dalton Transactions.

Induced Circular Dichroism of Polyoxometalates via Electrostatic Encapsulation with Chiral Organic Cations

Yizhan Wang, Lei Shi, Yang Yang, Bao Li,* Lixin Wu*

State Key Laboratory of Supramolecular Structure and Materials, College of Chemistry, Jilin University, Changchun 130012, P. R. China

*To whom correspondence should be addressed. E-mail: wulx@jlu.edu.cn.

Synthesis of chiral organic cations (R-, S-C_0, (R)- or (S)-N,N,N-trimethyl-1-phenylethanaminium iodide): An amount of 0.1 mL of CH_3I was added to a solution of 0.15 mL of R- or S- N,N-dimethyl-1-phenylethylamine in 1 mL of methanol. The reaction mixture was kept under stirring at room temperature for 48 h. The iodide salt was precipitated from methanol by adding Et_2O, filtered, and washed with Et_2O. The precipitate was dried under vacuum, giving the products, R-C_0 and S-C_0. For R-C_0: ^{1}H NMR (500 MHz, DMSO-d_6, TMS, ppm): δ = 1.73 (3 H, d, J = 6.8 Hz), 2.99 (9 H, s), 4.82 (1 H, m), 7.52 (3 H, m), 7.61 (2 H, m). For S-C_0: ^{1}H NMR (500 MHz, DMSO-d_6, TMS, ppm): δ = 1.72 (3 H, d, J = 6.8 Hz), 2.98 (9 H, s), 4.77 (1 H, m), 7.52 (3 H, m), 7.60 (2 H, m). MALDI-TOF MS: m/z: 165.15.

Synthesis of chiral organic cation (R-C_5, (R)-N,N,N-trimethyl-5-oxo-5-(1-phenylethoxy)pentan-1-aminium bromide): A mixture of (R)-(+)-1-phenyl ethanol (1.0 g), 5-bromovaleric acid (1.23 g), N,N'-dicyclohexylcarbodiimide (2.11 g), and 4-dimethylaminopyridine in dry dichloromethane (50 mL) was stirred for 48 h with the exclusion of moisture at room temperature. The resulting mixture was filtered and the filtrate was then evaporated under the reduce pressure. The residue was purified by column chromatography (20/1 of petroleum ether: ethyl acetate in volume ratio), giving the product of esterification. Then the mixture of esterification product (0.13 g) and trimethylamine (0.7 mL, 30% aqueous solution) in ethanol (50 mL) was refluxed for 48 h. The resulting mixture was evaporated under the reduce pressure. The residue was washed with diethyl ether (3 × 20 mL). Then the resulting solid was dissolved in 5 mL water, and extracted by dichloromethane three times (30 mL × 3). The organic phase was collected and evaporated under the reduce pressure, giving the chiral product R-C_5: ^{1}H NMR (500 MHz, DMSO-d_6, TMS, ppm): δ = 1.49 (3 H, d, J = 6.8 Hz), 1.53 (2 H, m), 1.68 (2 H, m), 2.43 (2 H, t), 3.01 (9 H, s), 3.28 (2 H, m), 5.82 (1 H, dd), 7.29−7.38 (5 H, m). MALDI-TOF MS: m/z: 265.10.

Synthesis of chiral organic cation (R-C_{11}, (R)-N,N,N-trimethyl-11-oxo-11-(1-phenylethoxy)undecan-1-aminium bromide): A mixture of (R)-(+)-1-phenyl ethanol (0.505 g), 11-bromoundecanoic acid (0.91 g), N,N'-dicyclohexylcarbodiimide (1.06 g), and 4-dimethylaminopyridine in dry dichloromethane (40 mL) was stirred for 48 h with the exclusion of moisture at room temperature. The resulting mixture was filtered and the filtrate was then

evaporated under the reduce pressure. The residue was purified by column chromatography (20/1 of petroleum ether/ethyl acetate in volume ratio), giving the product of esterification. Then the mixture of esterification product (0.13 g) and trimethylamine (0.5 mL, 30% aqueous solution) in ethanol (50 mL) was refluxed for 48 h and then evaporated under the reduce pressure. The residue was washed with diethyl ether (3 × 20 mL), giving the white solid R-C_{11}: ^{1}H NMR (500 MHz, DMSO-d_6, TMS, ppm): δ = 1.24 (12 H, m), 1.45 (3 H, d, J = 6.6 Hz),1.52 (2 H, m), 1.66 (2 H, m), 2.32 (2 H, t), 3.05 (9 H, s), 3.27 (2 H, m), 5.81 (1 H, dd), 7.35 (5 H, m). MALDI-TOF MS: m/z: 349.08.

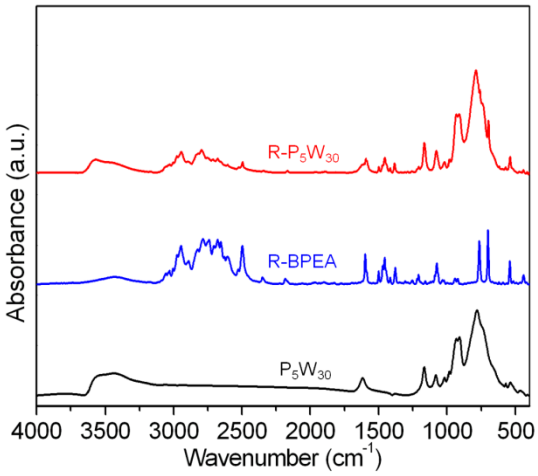

Figure S1. IR spectra of P_5W_{30} ($K_{12.5}Na_{1.5}[NaP_5W_{30}O_{110}]\cdot nH_2O$) (bottom), R-BPEA (middle) and R-P_5W_{30} (top) in KBr pellets.

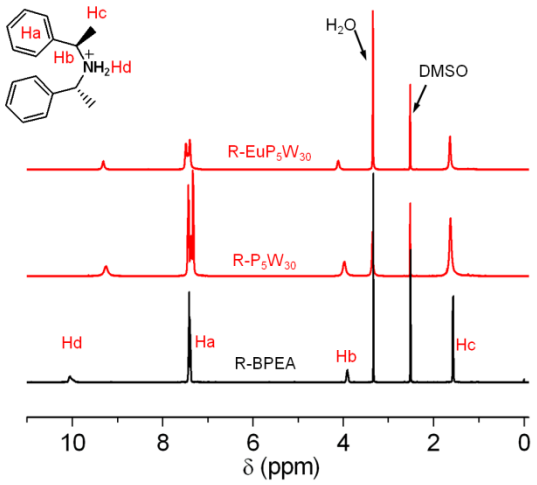

Figure S2. ^{1}H NMR spectra of R-BPEA, R-P_5W_{30} and R-EuP_5E_{30} in DMSO-d_6.

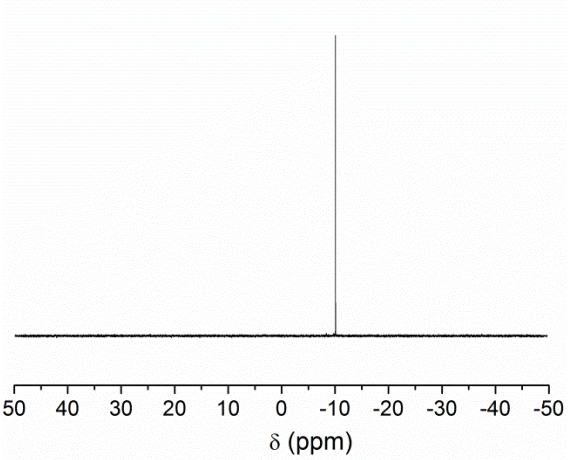

Figure S3. ^{31}P NMR spectra of R-P_5W_{30} in CD_3CN.

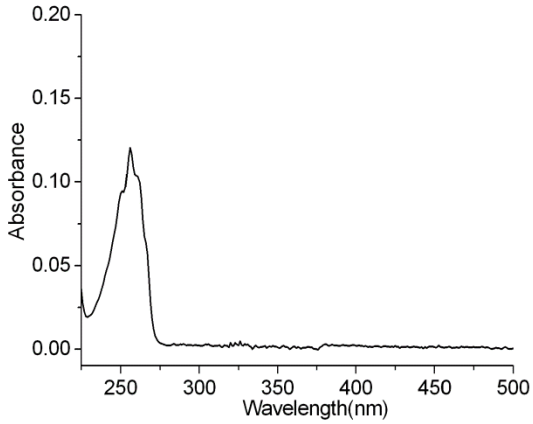

Figure S4. UV-Vis spectrum of R-BPEA in CH_3CN.

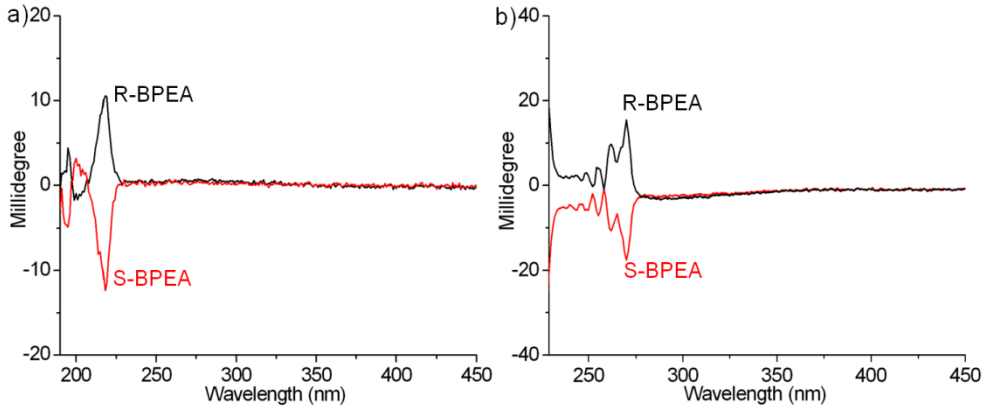

Figure S5. CD spectra of R- and S-BPEA in CH_3CN at a) c = 3×10^{-4} mol L^{-1}, l = 1 mm; and b) c = 3.8×10^{-3} mol L^{-1}, l = 10 mm.

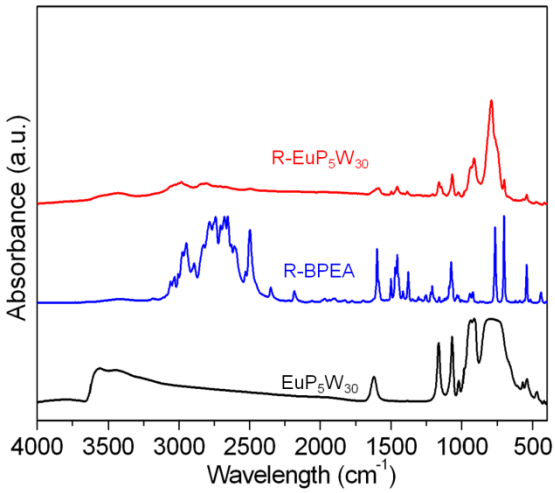

Figure S6. IR spectra of EuP_5W_{30} ($K_{12}[EuP_5W_{30}O_{110}]\cdot nH_2O$) (bottom), R-BPEA (middle) and R-EuP_5W_{30} (top) in KBr pellets.

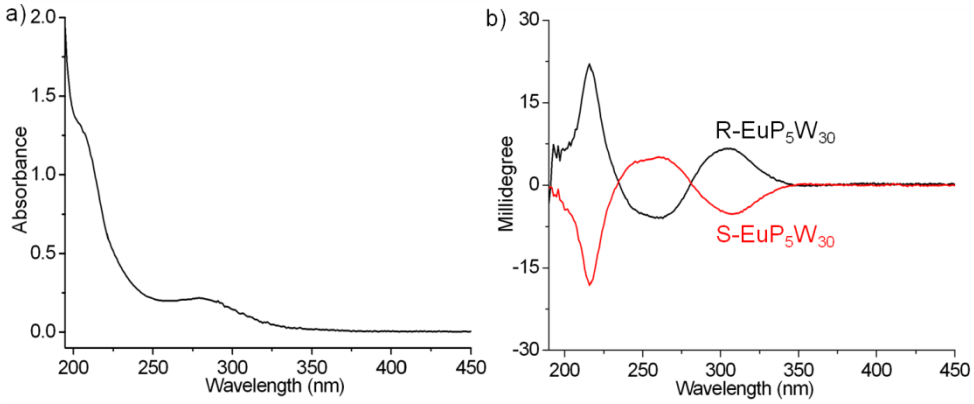

Figure S7. a) UV spectrum of R-EuP_5W_{30} in CH_3CN and b) CD spectra of R-EuP_5W_{30} and S-EuP_5W_{30} in CH_3CN at c= 1.9×10^{-5} mol L^{-1}, l = 1 mm.

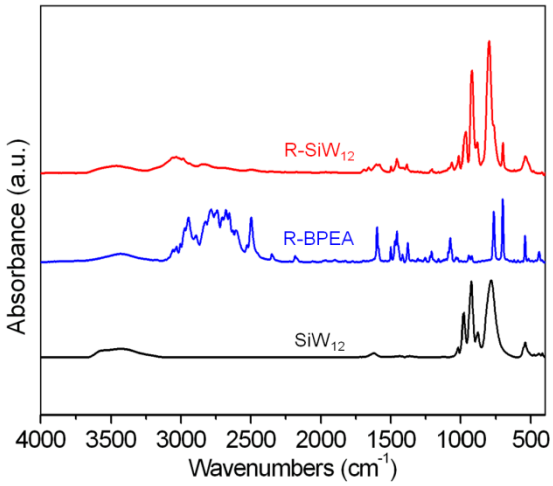

Figure S8. IR spectra of SiW_{12} ($H_4SiW_{12}O_{40}$) (bottom), R-BPEA (middle) and R-SiW_{12} (top) in KBr pellets.

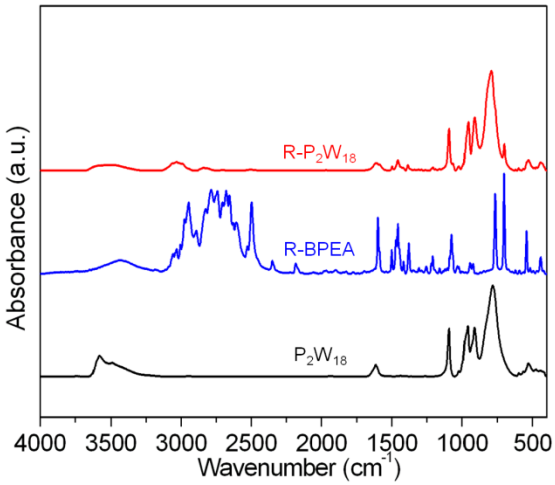

Figure S9. IR spectra of P_2W_{18} ($K_6P_2W_{18}O_{62}$) (bottom), R-BPEA (middle) and R-P_2W_{18} (top) in KBr pellets.

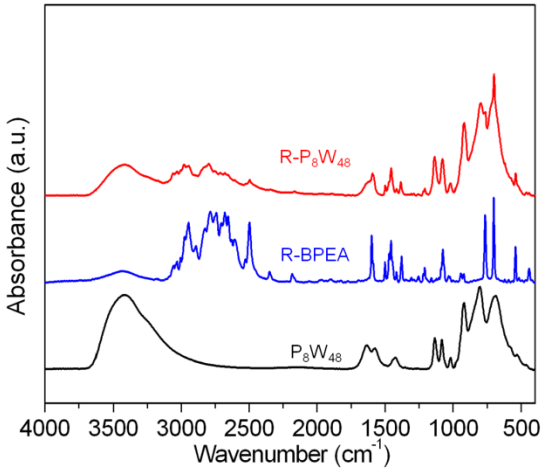

Figure S10. IR spectra of P_8W_{48} ($K_{28}Li_5H_7[P_8W_{48}O_{184}]\cdot 92H_2O$) (bottom), R-BPEA (middle) and R- P_8W_{48} (top) in KBr pellets.

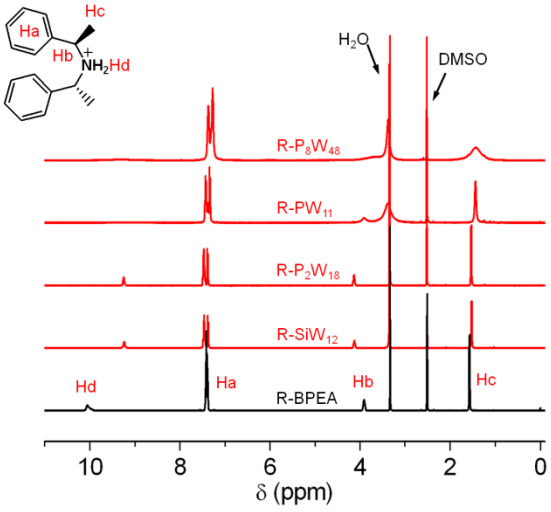

Figure S11. ^{1}H NMR spectra of R-BPEA, R-SiW_{12}, R-P_2W_{18}, R-PW_{11}, and R-P_8W_{48} in DMSO-d_6.

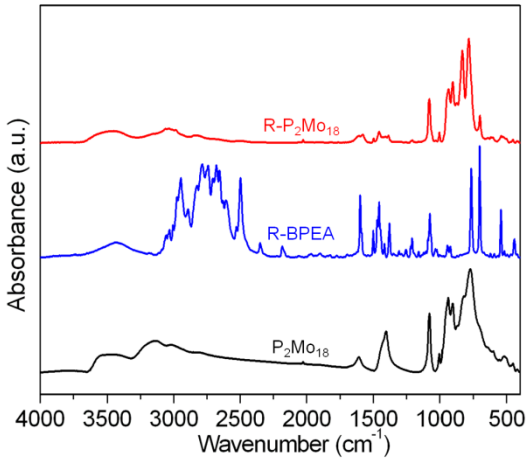

Figure S12. IR spectra of P_2Mo_{18} ($(NH_4)_6[P_2Mo_{18}O_{62}]\cdot 12H_2O$) (bottom), R-BPEA (middle), and R-P_2Mo_{18} (top) in KBr pellets.

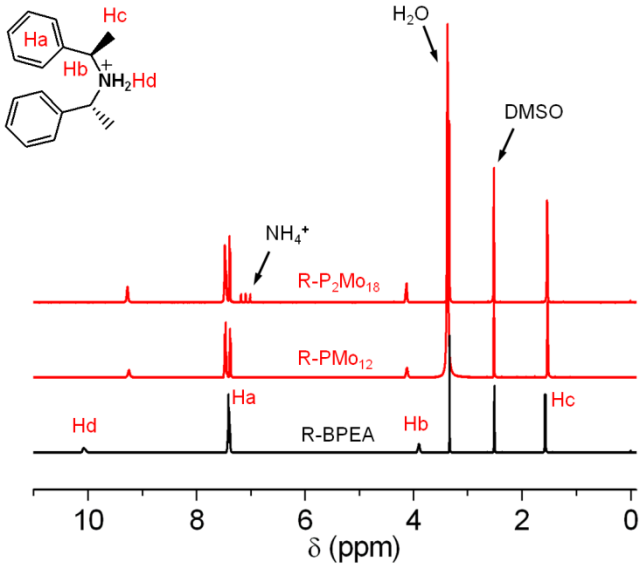

Figure S13. ^1H NMR spectra of R-BPEA, R-PMo_{12}, and R-P_2Mo_{18} in DMSO-d_6.

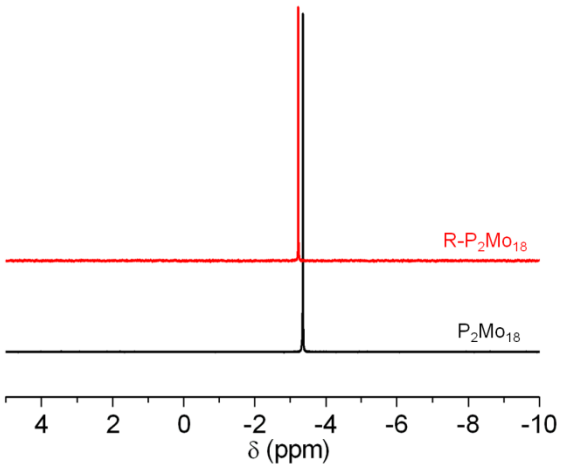

Figure S14. ^{31}P NMR spectra of P_2Mo_{18} and R-P_2Mo_{18} in CD_3CN.

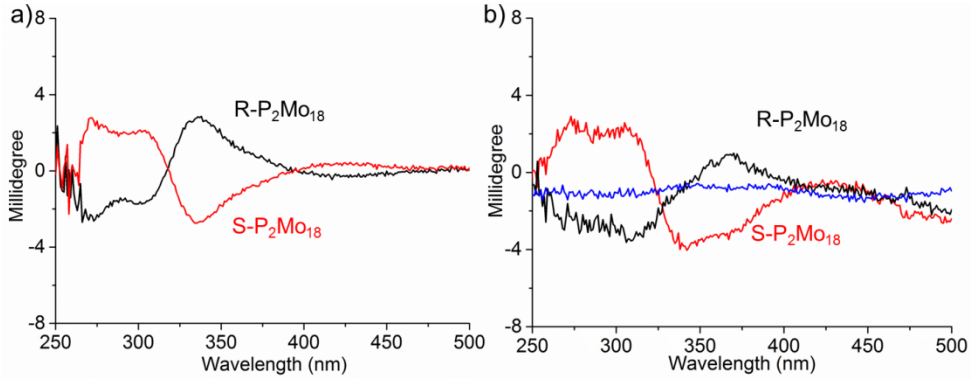

Figure S15. CD spectra of R-P_2Mo_{18} and S-P_2Mo_{18} a) in CH_3OH (c = 0.2 mg mL^{-1}, *l* = 1 mm); b) in solid KBr pellets (the blue line is the spectrum of KBr).

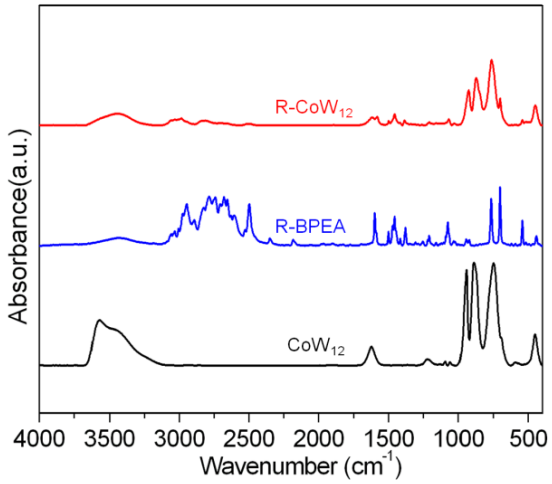

Figure S16. IR spectra of CoW_{12} ($K_6CoW_{12}O_{40}$) (bottom), R-BPEA (middle) and R-CoW_{12} (top) in KBr pellets.

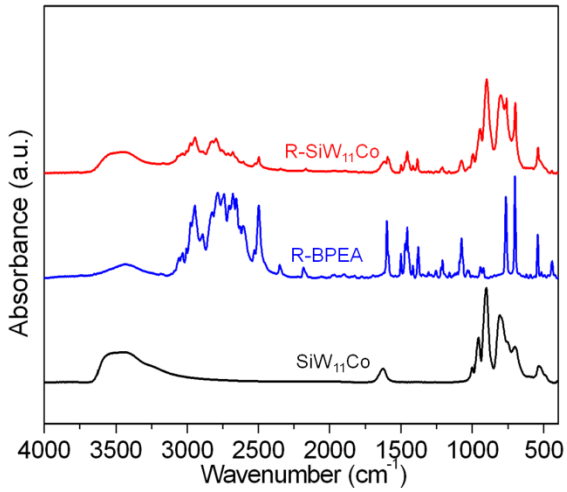

Figure S17. IR spectra of $SiW_{11}Co$ ($K_6SiW_{11}CoO_{39}$) (bottom), R-BPEA (middle) and R-$SiW_{11}Co$ (top) in KBr pellets.

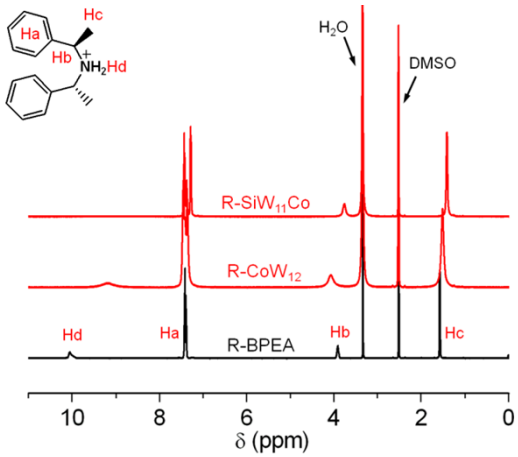

Figure S18. ^{1}H NMR spectra of R-BPEA, R-CoW_{12} and R-$SiW_{11}Co$ in DMSO-d_6.

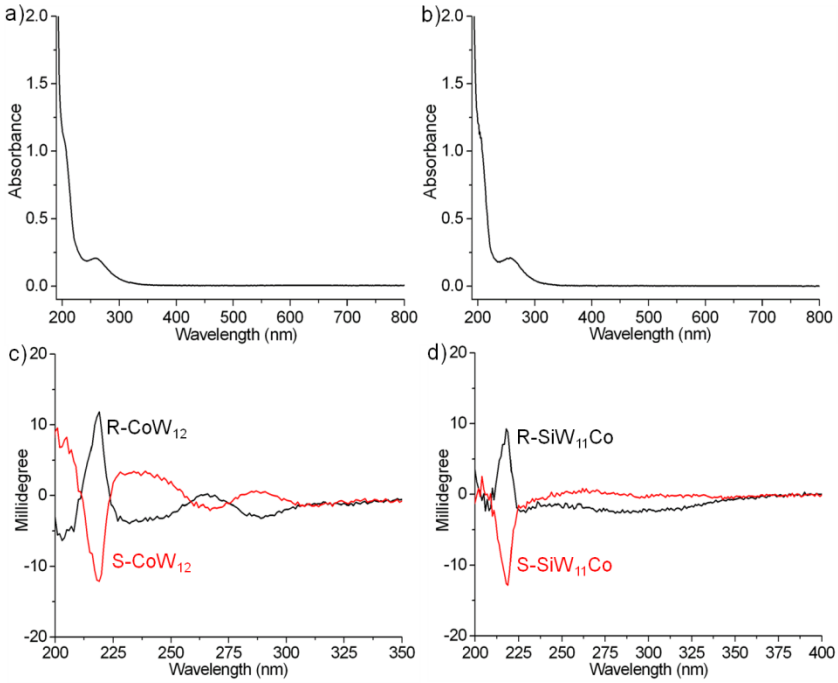

Figure S19. UV-Vis spectra of a) R-CoW_{12}, b) R-$SiW_{11}Co$, and CD spectra of c) R-,S-CoW_{12}, d) R-,S-$SiW_{11}Co$ in CH_3CN at c = 0.2 mg mL^{-1}, l = 1 mm.

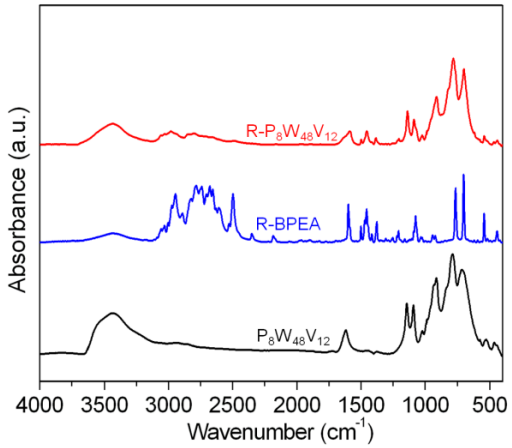

Figure S20. IR spectra of $P_8W_{48}V_{12}$ ($Na_{12}K_8H_4[K_8P_8W_{48}O_{184}(V_4V_2O_{12}(H_2O)_2)_2]$·ca.$80H_2O$) (bottom), R-BPEA (middle) and R-$P_8W_{48}V_{12}$ (top) in KBr pellets.

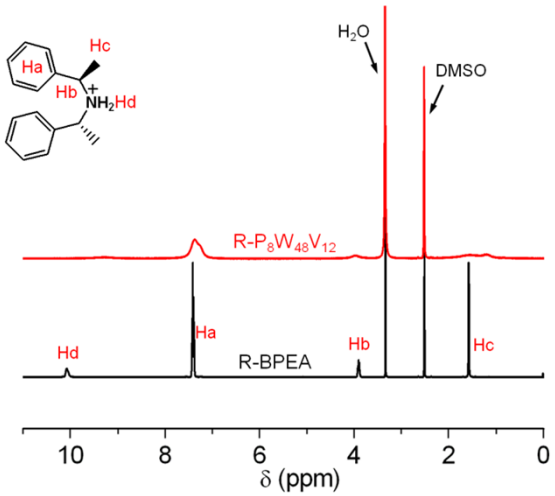

Figure S21. ^{1}H NMR spectra of R-BPEA and R-$P_8W_{48}V_{12}$ in DMSO-d_6.

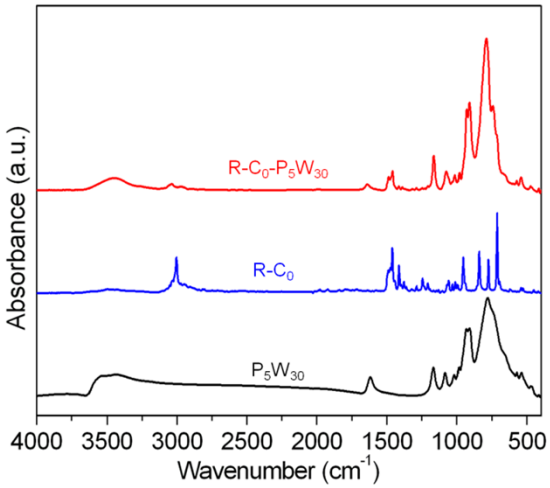

Figure S22. IR spectra of P_5W_{30} ($K_{12.5}Na_{1.5}[NaP_5W_{30}O_{110}]\cdot nH_2O$) (bottom), R-$C_0$ (middle) and R-C_0-P_5W_{30} (top) in KBr pellets.

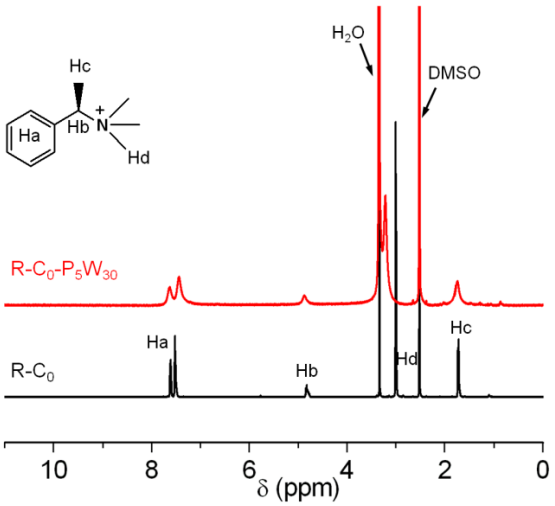

Figure S23. ^{1}H NMR spectra of R-C_0 and R-C_0-P_5W_{30} in DMSO-d_6.

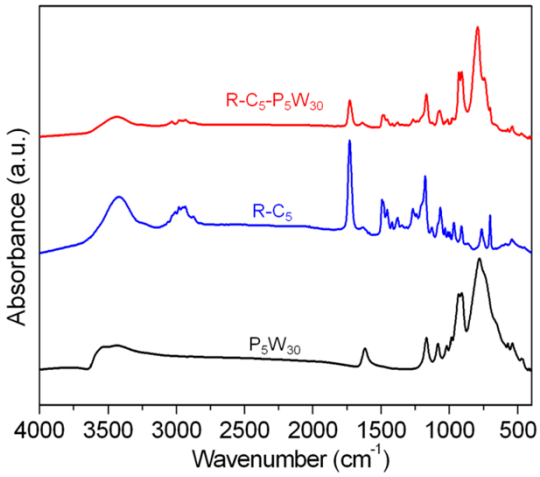

Figure S24. IR spectra of P_5W_{30} ($K_{12.5}Na_{1.5}[NaP_5W_{30}O_{110}]\cdot nH_2O$) (bottom), R-$C_5$ (middle) and R-C_5-P_5W_{30} (top) in KBr pellets.

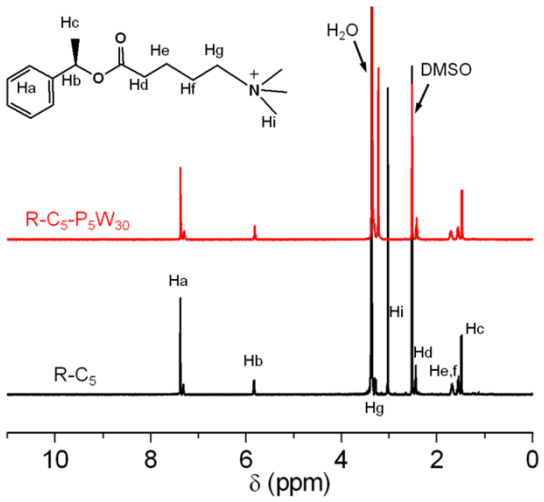

Figure S25. ^{1}H NMR spectra of R-C_5 and R-C_5-P_5W_{30} in DMSO-d_6.

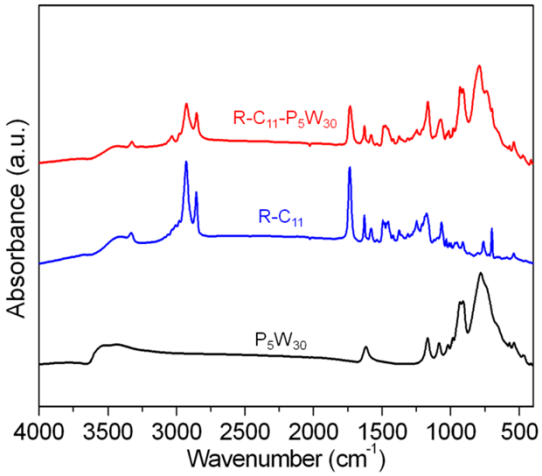

Figure S26. IR spectra of P_5W_{30} ($K_{12.5}Na_{1.5}[NaP_5W_{30}O_{110}]\cdot nH_2O$) (bottom), R-$C_{11}$ (middle) and R-C_{11}-P_5W_{30} (top) in KBr pellets.

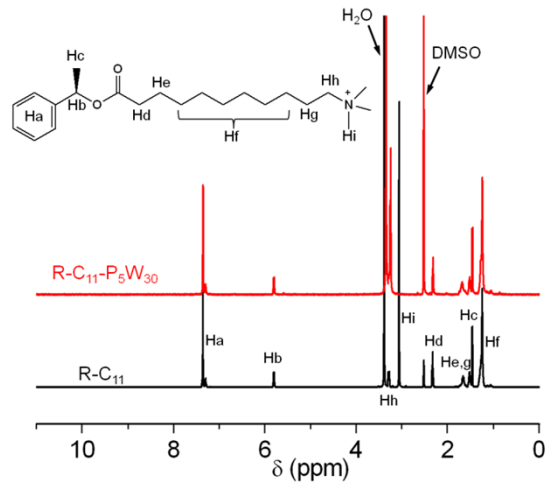

Figure S27. ^{1}H NMR spectra of R-C_{11} and R-C_{11}-P_5W_{30} in DMSO-d_6.

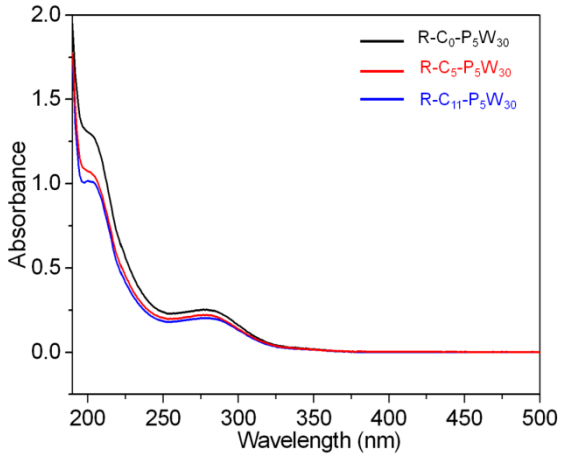

Figure S28. UV-Vis spectra of R-C_0-P_5W_{30}, R-C_5-P_5W_{30}, and R-C_{11}-P_5W_{30} in CH_3CN.

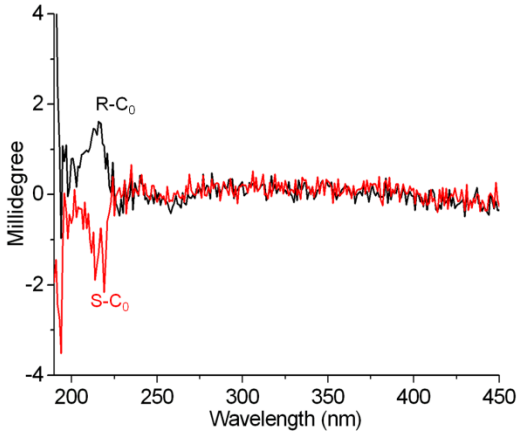

Figure S29. CD spectra of R-C_0 and S-C_0 in CH_3CN at c = 0.04 mg mL^{-1}, l = 1 mm.

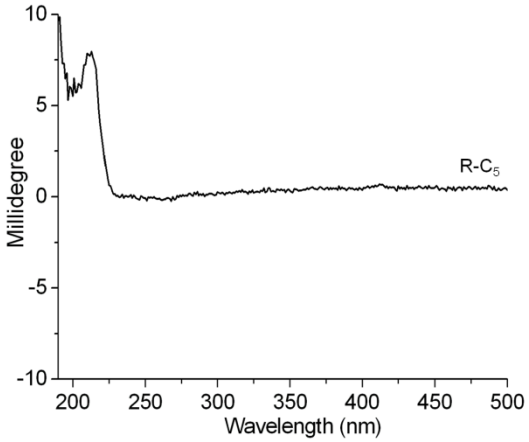

Figure S30. CD spectra of R-C_5 in CH_3CN at c= 0.2 mg mL^{-1}, l = 1 mm.

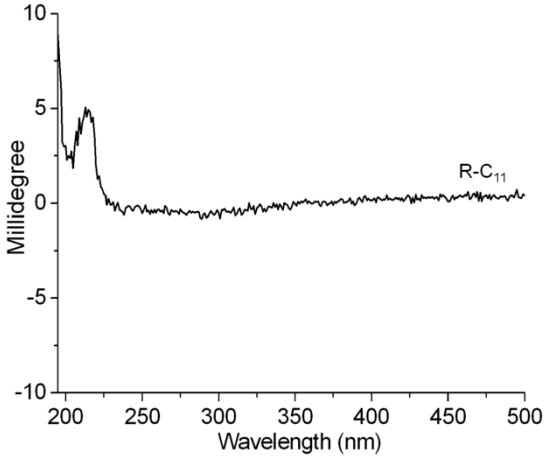

Figure S31. CD spectra of R-C_{11} in CH_3CN at c = 0.2 mg mL^{-1}, l = 1 mm.